University of Glasgow

Shamsudin, M.H., Rousseau, J., Verchery, G. and York, C.B. (2011) *Experimental validation of the mechanical coupling response for hygro-thermally curvature-stable laminated composite materials.* In: 6th International Conference "Supply on the wings" in conjunction with AIRTEC 2011, International Aerospace Supply Fair, 2-4 November 2011, Exhibition Center, Frankfurt / Main, Germany.

http://eprints.gla.ac.uk/56452/

Deposited on: 24 November 2011

Enlighten – Research publications by members of the University of Glasgow
http://eprints.gla.ac.uk

Experimental Validation of the Mechanical Coupling Response for Hygro-Thermally Curvature-Stable Laminated Composite Materials.

M. H. Shamsudin[1] and C.B. York[2]
School of Engineering, University of Glasgow, G12 8QQ Glasgow, Scotland, UK

J. Rousseau
Institut Supérieur de l'Automobile et des Transports Université de Bourgogne, Nevers, France

G. Verchery
Institut Supérieur des Matériaux et Mécaniques Avancés, Le Mans, France.

Stacking sequence configurations for hygro-thermally curvature-stable (HTCS) laminates have recently been identified in 9 classes of coupled laminate with standard ply angle orientations +45, −45, 0 and 90°. All arise from the judicious re-alignment of the principal material axis of parent classes with Bending-Twisting and/or Bending-Extension and Twisting-Shearing coupling; Off-axis material alignment of the principal material axis with respect to the structural or system axis for these parent classes gives rise to more complex combinations of mechanical coupling behaviour. The mechanical extension-twist coupling response of these two parent classes is assessed experimentally for 12-ply laminates to validate non-linear numerical simulations.

Nomenclature

A_{ij}	=	extensional (membrane) stiffness matrix and its elements (i,j = 1, 2, 6).
B_{ij}	=	bending-extension-coupling stiffness matrix and its elements (i,j = 1, 2, 6).
D_{ij}	=	bending (flexural) stiffness matrix and its elements (i,j = 1, 2, 6).
H	=	laminate thickness (= $n \times t$).
n	=	number of plies in laminate stacking sequence.
$\mathbf{N}$	=	in-plane force resultants (= $\{N_x,N_y,N_{xy}\}^T$).
N_x,N_y	=	in-plane axial load per unit length.
N_{xy}	=	in-plane shear flow.
$\mathbf{M}$	=	out-of-plane moment resultants (= $\{M_x,M_y,M_{xy}\}^T$).
M_x,M_y	=	bending moments per unit length about principal axes.
M_{xy}	=	twist moment per unit length.
Q_{ij}	=	reduced stiffness (i,j = 1, 2, 6).
Q'_{ij}	=	transformed reduced stiffness (i,j = 1, 2, 6).
t	=	ply thickness.
x,y,z	=	principal axes.
$\alpha_{Iso},\alpha_1,\alpha_2$	=	thermal expansion coefficients
β	=	off-axis alignment angle of principal fibre direction
$\boldsymbol{\varepsilon}$	=	in-plane strains (= $\{\varepsilon_x,\varepsilon_y,\gamma_{xy}\}^T$).
$\varepsilon_x,\varepsilon_y$	=	in-plane axial strains.
γ_{xy}	=	in-plane shear strain.
$\boldsymbol{\kappa}$	=	Curvatures (= $\{\kappa_x,\kappa_y,\kappa_{xy}\}^T$).
κ_x,κ_y	=	curvatures about principal axes.

[1] PhD Candidate, University of Glasgow, Glasgow.
[2] Corresponding Author: Christopher.York@Glasgow.ac.uk

κ_{xy}	=	twist curvature.
$\xi_{1\text{-}4}$	=	lamination parameters for extensional stiffness.
$\xi_{5\text{-}8}$	=	lamination parameters for coupling stiffness.
$\xi_{9\text{-}12}$	=	lamination parameters for bending stiffness.
+,−,±	=	angle plies, used in stacking sequence definition.
O,●	=	cross-plies, used in stacking sequence definition.

I. Introduction

Tailored composite laminates possessing complex mechanical couplings are beginning to find application beyond the aerospace sector, with which they have been traditionally associated, and towards new and emerging applications for which certification is less stringent and design rules have not become entrenched and risk averse. Indeed, recent research has demonstrated that there is a vast and unexplored laminate design space containing exotic forms of mechanical coupling on recently identified (York, 2010), which includes all interactions between Extension, Shearing, Bending and Twisting, and that a surprisingly broad range of these coupling responses can be achieved without the undesirable warping distortions that result from the high temperature curing process (York, 2011a/b); Such laminate designs may be described as hygro-thermally curvature-stable (HTCS) or warp-free.

One family of coupled laminate, with immunity to thermal warping (Nixon, 1987), has already been used extensively in tilt-rotor blade design. Here, extension-twisting coupling, at the structural or blade level, is used to develop an optimised twist distribution along the blade for both hover and forward flight: a change in rotor speed, and the resulting centrifugal forces, provides the required twist differential between the two flight regimes. This behaviour is achieved from laminate level extension-shearing coupling, but through off-axis alignment of a balanced and symmetric laminate. However, such laminate designs possess significant bending-twisting coupling at the laminate level, leading to detrimental effects on the compression buckling strength of the blade, which is an important static design constraint. In fact, improvements in the static buckling strength can be achieved, in the absence of laminate level bending-twisting coupling, and without affecting the bending-twisting response at the structural or wing-box level (York, 2008), but these laminates are neither balanced nor symmetric.

An alternative design for aero-elastic compliant rotor blades is through tailored extension-twist coupling at the laminate level (Winckler, 1985), which is an example of a laminate design that requires either specially curved tooling or HTCS properties in order to remain flat after high temperature curing.

Mechanical coupling behaviour offers great potential for applications in the aerospace sector, beyond those of rotating blades, but only if the constraint of the black metal design philosophy based on balanced and symmetric laminates can be overcome.

The motivation for this study arises from the fact that practical exploitation of mechanically coupled composite laminates presents a significant technical challenge due to the associated thermal warping distortions, which are an inevitable result of the high temperature curing process. However, whilst the requirements for achieving HTCS composite laminates with mechanically coupled properties have now been addressed extensively in the literature (Chen, 2003; Cross, et al. 2008; York, 2011a/b/c; Verchery, 2011a/b), few studies have considered mechanical coupling behaviour beyond that of the extension-twisting coupling mechanism first postulated by Winkler (1985).

Preliminary experimental validation results are reported here for representative samples from twenty-four classes of coupled laminate, the vast majority of which possess coupling behaviour not previously identified in the literature. A summary of the twenty-four classes are first presented, followed by details of the design rules for identifying the laminate classes possessing the HTCS condition. Numerical and experimental validation results are then presented for a small selection of HTCS laminate designs, which provide maximum mechanical coupling response with standard ply orientations. These results will begin to answer the fundamental question of whether alternative forms of mechanical coupling can be exploited to provide desirable structural response using a lighter (thinner) laminate design whilst satisfying the static (improved buckling strength) design constraint.

Characterisation of laminates

Laminated composite materials are typically characterized in terms of their response to mechanical and/or thermal loading, which is generally associated with a description of their coupling behaviour, not present in conventional materials, i.e., coupling between in-plane (i.e., extension or membrane) and out-of-plane (i.e., bending or flexure) responses when $B_{ij} \neq 0$ in Eq. (1), coupling between in-plane shear and extension when A_{16}, $A_{26} \neq 0$, and coupling between out-of-plane bending and twisting when D_{16}, $D_{26} \neq 0$.

$$\begin{Bmatrix} N_x \\ N_y \\ N_{xy} \end{Bmatrix} = \begin{bmatrix} A_{11} & A_{12} & A_{16} \\ & A_{22} & A_{26} \\ \text{Sym.} & & A_{66} \end{bmatrix} \begin{Bmatrix} \varepsilon_x \\ \varepsilon_y \\ \gamma_{xy} \end{Bmatrix} + \begin{bmatrix} B_{11} & B_{12} & B_{16} \\ & B_{22} & B_{26} \\ \text{Sym.} & & B_{66} \end{bmatrix} \begin{Bmatrix} \kappa_x \\ \kappa_y \\ \kappa_{xy} \end{Bmatrix}$$

$$\begin{Bmatrix} M_x \\ M_y \\ M_{xy} \end{Bmatrix} = \begin{bmatrix} B_{11} & B_{12} & B_{16} \\ & B_{22} & B_{26} \\ \text{Sym.} & & B_{66} \end{bmatrix} \begin{Bmatrix} \varepsilon_x \\ \varepsilon_y \\ \gamma_{xy} \end{Bmatrix} + \begin{bmatrix} D_{11} & D_{12} & D_{16} \\ & D_{22} & D_{26} \\ \text{Sym.} & & D_{66} \end{bmatrix} \begin{Bmatrix} \kappa_x \\ \kappa_y \\ \kappa_{xy} \end{Bmatrix} \quad (1)$$

where the force and moment resultant vector components account for the combined effects of mechanical, thermal and hygral loading. Whilst Eq. (1) describes the well-known **ABD** relation from classical lamination theory, it is more often expressed using compact notation:

$$\begin{Bmatrix} \mathbf{N} \\ \mathbf{M} \end{Bmatrix} = \begin{bmatrix} \mathbf{A} & \mathbf{B} \\ \mathbf{B} & \mathbf{D} \end{bmatrix} \begin{Bmatrix} \boldsymbol{\varepsilon} \\ \boldsymbol{\kappa} \end{Bmatrix} \quad (2)$$

The coupling behaviour, which is dependent on the form of the elements in each of the extensional (**A**), coupling (**B**) and bending (**D**) stiffness matrices can also be described by an extended subscript notation, defined previously by the Engineering Sciences Data Unit (ESDU, 1994): a fully populated extensional stiffness matrix (**A**) is denoted as $\mathbf{A}_F$, and implies that the laminate has coupling between extension and shearing and; a fully populated bending stiffness matrix (**D**), denoted as $\mathbf{D}_F$, implies that the laminate has bending-twisting coupling. These coupling responses arise from the none zero elements, A_{16}, A_{26} and D_{16}, D_{26}, as illustrated in Table 1(a) and (b), respectively. An absence of these elements, i.e. $A_{16} = A_{26} = D_{16} = D_{26} = 0$, results in uncoupled extensional (**A**) and bending (**D**) stiffness, as would be the case in a simple isotropic material. In the uncoupled case, the form of each matrix is denoted $\mathbf{A}_S$ and $\mathbf{D}_S$, respectively. The coupling matrix (**B**) exists in a number of different forms, see Table 1(c); each form having a major influence on the relationship between in-plane and out-of-plane response of a given laminate. The classical manufacturing technique of employing symmetric stacking sequences guarantees that the element of the coupling matrix $\mathbf{B} = 0$; denoted by $\mathbf{B}_0$. Therefore a balanced and symmetric laminate would be designated $\mathbf{A}_S\mathbf{B}_0\mathbf{D}_F$, indicating uncoupled or simple extensional stiffness matrix (**A**), a null coupling stiffness matrix (**B**) and bending-twisting coupling due to the fully populated bending stiffness matrix (**D**). Balanced and symmetric laminates with no (bending-twisting) coupling are described elsewhere (York, 2009).

The subscript notation was used to describe 10 classes of coupled composite laminate (ESDU, 1994), but recent research has revealed the existence of 24 unique classes (York, 2010), in which a response-based labelling was also introduced to aid the understanding on the coupled nature of a given laminate class, complementing the subscript notation, which describes the form of the **ABD** matrix, see Table 1. Based on the cause and effect relationship, an $A_FB_0D_F$ laminate would have the associated response-based labelling *E-S*;*B-T*, denoting that Extension will cause a Shearing effect (*E-S*), and bending will cause a twisting effect (*B-T*). Each cause and effect pair is underlined and is reversible. A semicolon is introduced to distinguish between couplings relating to the extensional (**A**), coupling (**B**) and bending (**D**) stiffness matrices, respectively.

Table 1 - Subscript notation, response based labelling and associated form of the: (a) extensional stiffness matrix, **A**; (b) coupling stiffness matrix, **B**, and; (c) bending stiffness matrix, **D**.

(a)

Subscript notation ESDU (1994)	Response-based labelling	Matrix form
$\mathbf{A}_S$	Simple laminate	$\begin{bmatrix} A_{11} & A_{12} & 0 \\ A_{21} & A_{22} & 0 \\ 0 & 0 & A_{66} \end{bmatrix}$
$\mathbf{A}_F$	Shear-Extension; *S-E*	$\begin{bmatrix} A_{11} & A_{12} & A_{16} \\ A_{21} & A_{22} & A_{26} \\ A_{61} & A_{62} & A_{66} \end{bmatrix}$

(b)

Subscript notation ESDU (1994)	Response-based labelling	Matrix form
$\mathbf{D}_S$	Simple laminate	$\begin{bmatrix} D_{11} & D_{12} & 0 \\ D_{21} & D_{22} & 0 \\ 0 & 0 & D_{66} \end{bmatrix}$
$\mathbf{D}_F$	Twisting-Bending; *T-B*	$\begin{bmatrix} D_{11} & D_{12} & D_{16} \\ D_{21} & D_{22} & D_{26} \\ D_{61} & D_{62} & D_{66} \end{bmatrix}$

(c)

Subscript notation ESDU (1994)	Response-based labelling	Matrix form
$\mathbf{B}_l$	Extension-Bending; *E-B*	$\begin{bmatrix} B_{11} & 0 & 0 \\ 0 & B_{22} & 0 \\ 0 & 0 & 0 \end{bmatrix}$
$\mathbf{B}_t$	Extension-Twisting and Shearing-Bending; *E-T-S-B*	$\begin{bmatrix} 0 & 0 & B_{16} \\ 0 & 0 & B_{26} \\ B_{61} & B_{62} & 0 \end{bmatrix}$
$\mathbf{B}_{lt}$	Extension-Bending, Extension-Twisting and Shearing-Bending; *E-B-E-T-S-B*	$\begin{bmatrix} B_{11} & 0 & B_{16} \\ 0 & B_{22} & B_{26} \\ B_{61} & B_{62} & 0 \end{bmatrix}$
$\mathbf{B}_S$	Extension-Bending and Shearing-Twisting; *E-B-S-T*	$\begin{bmatrix} B_{11} & B_{12} & 0 \\ B_{21} & B_{22} & 0 \\ 0 & 0 & B_{66} \end{bmatrix}$
$\mathbf{B}_F$	Extension-Bending, Shearing-Bending, Extension-Twisting, and Shearing-Twisting; *E-B-S-B-E-T-S-T*	$\begin{bmatrix} B_{11} & B_{12} & B_{16} \\ B_{21} & B_{22} & B_{26} \\ B_{61} & B_{62} & B_{66} \end{bmatrix}$

The illustrations presented in Figs 1 - 4 represent the thermal (contraction) response of initially flat laminates after a typical elevated temperature curing process for all 24 unique classes of coupled laminate. Figures 1 and 2 contain combinations that are extensionally uncoupled, i.e. all designations begin with $\mathbf{A}_S$, whilst Figs 3 and 4 contain combinations with shearing-extension coupling, i.e., all designations begin with $\mathbf{A}_F$. Laminates in Figs 1 and 4 are uncoupled in bending ($\mathbf{D}_S$), whereas Figs 2 and 3 contain combinations with bending-twisting coupling ($\mathbf{D}_F$). The complex forms of the coupling (**B**) stiffness matrix appear in the same (column) location in each figure, beginning and ending with the fully uncoupled ($\mathbf{B}_0$) and fully coupled form ($\mathbf{B}_F$), respectively. The example stacking sequences adjacent to each illustration are representative of the minimum ply number grouping for each laminate class; for angle ply laminates with or without cross plies, where symbols +, -, O, ● represent standard angle ply orientations +45, -45, 0 and 90°, respectively.

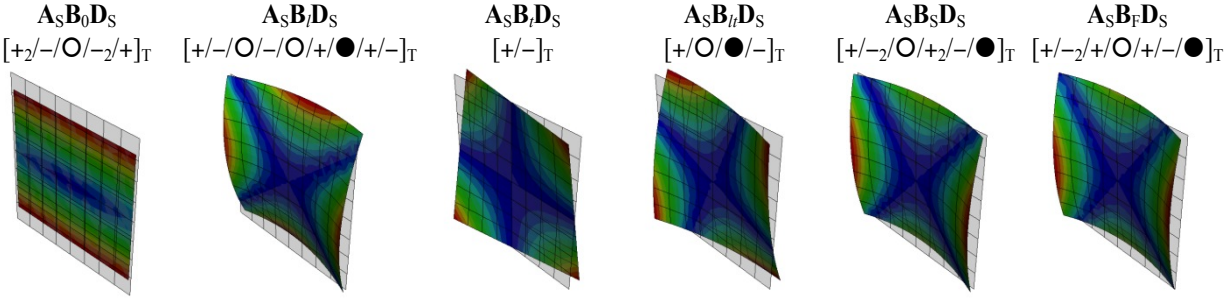

Figure 1 - Isolated coupling responses, due to free thermal contraction, for: ($\mathbf{A_SB_0D_S}$) Simple or uncoupled laminate; ($\mathbf{A_SB_lD_S}$) *B-E* laminate with bending-extension coupling; ($\mathbf{A_SB_tD_S}$) *B-S*-*T-E* laminate with bending-shearing and twisting-extension coupling; ($\mathbf{A_SB_{lt}D_S}$) *B-E*-*B-S*-*T-E* laminate with bending-extension, bending-shearing and twisting-extension coupling; ($\mathbf{A_SB_SD_S}$) *B-E*-*T-S* laminate with bending-extension and twisting-shearing coupling and; ($\mathbf{A_SB_FD_S}$) *B-E*-*B-S*-*T-E*-*T-S* or fully coupled laminate.

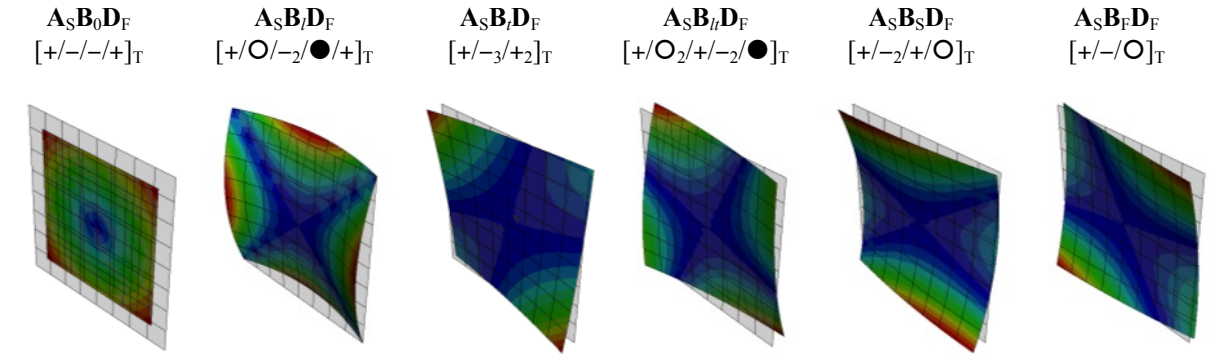

Figure 2 - Coupling responses, due to free thermal contraction, for ($A_FB_0D_F$) *E-S*;*B-T* laminates with extension-shearing and bending-twisting coupling combined with: ($A_FB_lD_F$) *B-E* or bending-extension coupling; ($A_FB_tD_F$) *B-S*-*T-E* or bending-shearing and twisting-extension coupling; ($A_FB_{lt}D_F$) *B-E*-*B-S*-*T-E* or bending-extension, bending-shearing and twisting-extension coupling; ($A_FB_SD_F$) *B-E*-*T-S* or bending-extension and twisting-shearing coupling and; ($A_FB_FD_F$) *B-E*-*B-S*-*T-E*-*T-S* or fully coupled laminate.

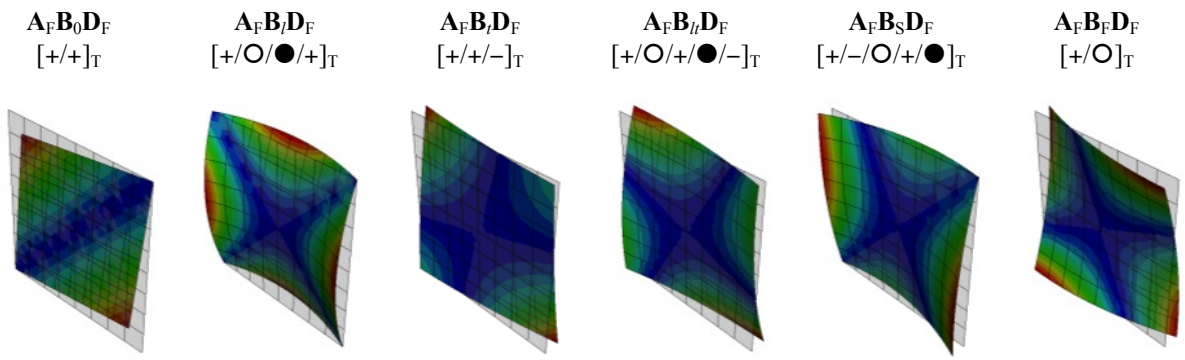

Figure 3 - Coupling responses, due to free thermal contraction, for ($A_FB_0D_F$) *E-S*;*B-T* laminates with extension-shearing and bending-twisting coupling combined with: ($A_FB_lD_F$) *B-E* or bending-extension coupling; ($A_FB_tD_F$) *B-S*-*T-E* or bending-shearing and twisting-extension coupling; ($A_FB_{lt}D_F$) *B-E*-*B-S*-*T-E* or bending-extension, bending-shearing and twisting-extension coupling; ($A_FB_SD_F$) *B-E*-*T-S* or bending-extension and twisting-shearing coupling and; ($A_FB_FD_F$) *B-E*-*B-S*-*T-E*-*T-S* or fully coupled laminate.

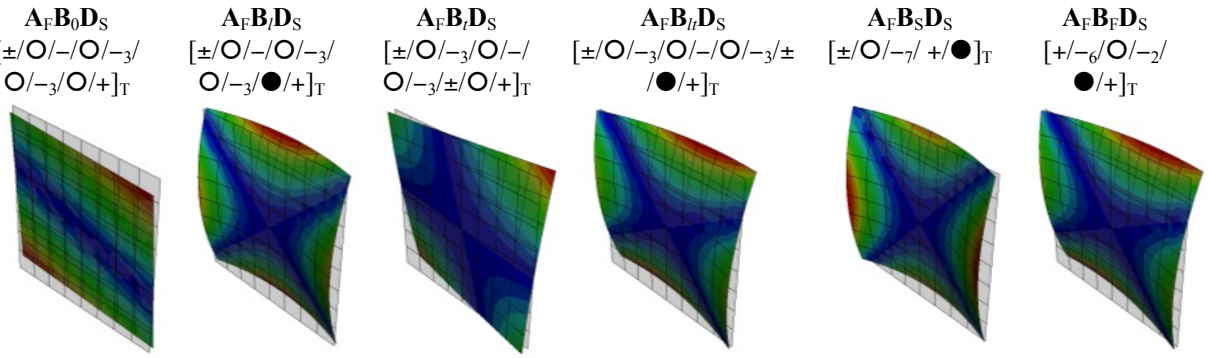

Figure 4 - Coupling responses, due to free thermal contraction, for ($A_FB_0D_S$) *E-S* laminates with extension-shearing coupling combined with: ($A_FB_lD_S$) *B-E* or bending-extension coupling; ($A_FB_tD_S$) *B-S*-*T-E* or bending-shearing and twisting-extension coupling; ($A_FB_{lt}D_S$) *B-E*-*B-S*-*T-E* or bending-extension, bending-shearing and twisting-extension coupling; ($A_FB_SD_S$) *B-E*-*T-S* or bending-extension and twisting-shearing coupling and; ($A_FB_FD_S$) *B-E*-*B-S*-*T-E*-*T-S* or fully coupled laminate.

II. Verification of Hygrothermally Curvature Stable (HTCS) Laminates

Winckler (1985) is credited with being the first to discover a HTCS laminate solution: an eight-ply configuration, developed using the concept of bonding two (or more) symmetric cross-ply $[O/\bullet/\bullet/O]_T$ sub-laminates, where each sub-laminate is counter-rotated by $\pi/8$, giving rise to the laminate: $[22.5/-67.5_2/22.5/-22.5/67.5_2/-22.5]_T$, which possesses Extension-Twisting and Shearing-Bending coupling. The symmetric cross-ply sub-laminate represents a hygro-thermally curvature-stable configuration, which remains so after rotation and/or combining with additional sub-laminates through stacking or interlacing.

The conditions for hygro-thermally curvature-stable behaviour are achieved through square symmetry in **A**, **B** and $\mathbf{N}^{th}$, with $\mathbf{M}^{th} = \mathbf{0}$ (Verchery, 2001a), where square symmetry is defined (Tsai and Hahn, 1980) as equal stiffness on principal axes, as would be the case in a cross-ply laminate or a fabric with balanced weave.

The **ABD** stiffness matrix and the thermal force ($\mathbf{N}^{th}$) and moment ($\mathbf{M}^{th}$) vectors can be calculated, from the laminate invariants and lamination parameters, using Eqs (3) and (4) respectively.

$$
\begin{aligned}
A_{11} &= \{U_1 + \xi_1 U_2 + \xi_2 U_3\} \times H \\
A_{12} &= A_{21} = \{-\xi_2 U_3 + U_4\} \times H \\
A_{16} &= A_{61} = \{\xi_3 U_2/2 + \xi_4 U_3\} \times H \\
A_{22} &= \{U_1 - \xi_1 U_2 + \xi_2 U_3\} \times H \\
A_{26} &= A_{62} = \{\xi_3 U_2/2 - \xi_4 U_3\} \times H \\
A_{66} &= \{-\xi_2 U_3 + U_5\} \times H
\end{aligned}
\qquad
\begin{aligned}
B_{11} &= \{\xi_5 U_2 + \xi_6 U_3\} \times H^2/4 \\
B_{12} &= B_{21} = \{-\xi_6 U_3\} \times H^2/4 \\
B_{16} &= B_{61} = \{\xi_7 U_2/2 + \xi_8 U_3\} \times H^2/4 \\
B_{22} &= \{-\xi_5 U_2 + \xi_6 U_3\} \times H^2/4 \\
B_{26} &= B_{62} = \{\xi_7 U_2/2 - \xi_8 U_3\} \times H^2/4 \\
B_{66} &= \{-\xi_6 U_3\} \times H^2/4
\end{aligned}
\qquad
\begin{aligned}
D_{11} &= \{U_1 + \xi_9 U_2 + \xi_{10} U_3\} \times H^3/12 \\
D_{12} &= D_{21} = \{U_4 - \xi_{10} U_3\} \times H^3/12 \\
D_{16} &= D_{61} = \{\xi_{11} U_2/2 + \xi_{12} U_3\} \times H^3/12 \\
D_{22} &= \{U_1 - \xi_9 U_2 + \xi_{10} U_3\} \times H^3/12 \\
D_{26} &= D_{62} = \{\xi_{11} U_2/2 - \xi_{12} U_3\} \times H^3/12 \\
D_{66} &= \{-\xi_{10} U_3 + U_5\} \times H^3/12
\end{aligned}
\tag{3}
$$

$$
N^{th} = \begin{Bmatrix} N_x^{th} \\ N_y^{th} \\ N_{xy}^{th} \end{Bmatrix} = \frac{1}{2} \begin{Bmatrix} (U_1+U_4)(\alpha_1+\alpha_2) + U_2(\alpha_1-\alpha_2) + \xi_1 \left[U_2(\alpha_1+\alpha_2) + (U_1+2U_3-U_4)(\alpha_1-\alpha_2) \right] \\ (U_1+U_4)(\alpha_1+\alpha_2) + U_2(\alpha_1-\alpha_2) - \xi_1 \left[U_2(\alpha_1+\alpha_2) + (U_1+2U_3-U_4)(\alpha_1-\alpha_2) \right] \\ \xi_3 \left[U_2(\alpha_1+\alpha_2) + (U_1+2U_3-U_4)(\alpha_1-\alpha_2) \right] \end{Bmatrix} \Delta T
$$

$$
M^{th} = \begin{Bmatrix} M_x^{th} \\ M_y^{th} \\ M_{xy}^{th} \end{Bmatrix} = \frac{1}{2} \begin{Bmatrix} \xi_5 \left[U_2(\alpha_1+\alpha_2) + (U_1+2U_3-U_4)(\alpha_1-\alpha_2) \right] \\ -\xi_5 \left[U_2(\alpha_1+\alpha_2) + (U_1+2U_3-U_4)(\alpha_1-\alpha_2) \right] \\ \xi_7 \left[U_2(\alpha_1+\alpha_2) + (U_1+2U_3-U_4)(\alpha_1-\alpha_2) \right] \end{Bmatrix} \Delta T
\tag{4}
$$

Where the laminate invariants are given by:

$$
\begin{aligned}
U_1 &= \{3Q_{11} + 3Q_{22} + 2Q_{12} + 4Q_{66}\}/8 \\
U_2 &= \{Q_{11} - Q_{22}\}/2 \\
U_3 &= \{Q_{11} + Q_{22} - 2Q_{12} - 4Q_{66}\}/8 \\
U_4 &= \{Q_{11} + Q_{22} + 6Q_{12} - 4Q_{66}\}/8 \\
U_5 &= \{Q_{11} + Q_{22} - 2Q_{12} + 4Q_{66}\}/8
\end{aligned}
\tag{5}
$$

And the lamination parameters by:

$$
\begin{aligned}
\xi_1 &= \sum_{k=1}^{n} \cos 2\theta_k (z_k - z_{k-1}) \\
\xi_2 &= \sum_{k=1}^{n} \cos 4\theta_k (z_k - z_{k-1}) \\
\xi_3 &= \sum_{k=1}^{n} \sin 2\theta_k (z_k - z_{k-1}) \\
\xi_4 &= \sum_{k=1}^{n} \sin 4\theta_k (z_k - z_{k-1})
\end{aligned}
\qquad
\begin{aligned}
\xi_5 &= \sum_{k=1}^{n} \cos 2\theta_k (z_k^2 - z_{k-1}^2)/2 \\
\xi_6 &= \sum_{k=1}^{n} \cos 4\theta_k (z_k^2 - z_{k-1}^2)/2 \\
\xi_7 &= \sum_{k=1}^{n} \sin 2\theta_k (z_k^2 - z_{k-1}^2)/2 \\
\xi_8 &= \sum_{k=1}^{n} \sin 4\theta_k (z_k^2 - z_{k-1}^2)/2
\end{aligned}
\qquad
\begin{aligned}
\xi_9 &= \sum_{k=1}^{n} \cos 2\theta_k (z_k^3 - z_{k-1}^3)/3 \\
\xi_{10} &= \sum_{k=1}^{n} \cos 4\theta_k (z_k^3 - z_{k-1}^3)/3 \\
\xi_{11} &= \sum_{k=1}^{n} \sin 2\theta_k (z_k^3 - z_{k-1}^3)/3 \\
\xi_{12} &= \sum_{k=1}^{n} \sin 4\theta_k (z_k^3 - z_{k-1}^3)/3
\end{aligned}
\tag{6}
$$

Finally, the reduced stiffness terms are calculated from the material properties:

$$
\begin{aligned}
Q_{11} &= E_1/(1 - \nu_{12}\nu_{21}), \; Q_{12} = \nu_{12}E_2/(1 - \nu_{12}\nu_{21}) \\
Q_{22} &= E_2/(1 - \nu_{12}\nu_{21}), \; Q_{66} = G_{12}
\end{aligned}
\tag{7}
$$

A. Hygro-Thermally Curvature Stable Stacking Sequences.

Stacking sequences have been selected for 12 ply laminates, which have previously been identified as hygro-thermally curvature-stable (York, 2010b). Laminates 25 and 27 are both from the parent $\mathbf{A_S B_S D_S}$ laminate classes, from which other coupled conditions are derivable through off-axis alignment. The stacking sequences are given in Table 2.

Table 2 – 12-ply hygro-thermally curvature-stable laminates

	Stacking Sequence
Laminate 25	$\mathbf{A_S B_S D_S}$: $[-45/45/45/0/-45/-45/45/90/90/90/0/0]_T$
Laminate 27	$\mathbf{A_S B_S D_S}$: $[-45/45/45/-45/45/-45/-45/45/90/0/0/90]_T$

The non-dimensional parameters, ξ_i, are independent of the material properties but are ply orientation dependent, see Table 3. This material independence extends to the form of the **ABD** matrix for identifying square symmetry, i.e., the HTCS condition demonstrated in Eq. (8)

Table 3 – Lamination parameters for Laminate 27

	Extensional Matrix (A)				Coupling Matrix (B)				Bending Matrix (D)			
	ξ_1	$\boldsymbol{\xi_2}$	ξ_3	ξ_4	ξ_5	$\boldsymbol{\xi_6}$	ξ_7	ξ_8	ξ_9	ξ_{10}	ξ_{11}	ξ_{12}
Laminate 25	0.00	**0.00**	0.00	0.00	0.00	**0.83**	0.00	0.00	0.25	0.08	0.00	0.00
Laminate 27	0.00	**-0.33**	0.00	0.00	0.00	**0.89**	0.00	0.00	-0.03	-0.04	0.00	0.00

$$A=\begin{bmatrix} A_{11} & A_{12} & 0 \\ A_{21} & A_{11} & 0 \\ 0 & 0 & A_{66} \end{bmatrix} \quad B=\begin{bmatrix} B_{11} & -B_{11} & 0 \\ -B_{11} & B_{11} & 0 \\ 0 & 0 & -B_{11} \end{bmatrix} \quad D=\begin{bmatrix} D_{11} & D_{12} & 0 \\ D_{21} & D_{22} & 0 \\ 0 & 0 & D_{66} \end{bmatrix} \tag{8}$$

Equation (8) defines the form of the **ABD** matrix for both laminates. However, laminate 25 is extensionally isotropic, i.e. $A_{66} = (A_{11} - A_{12})/2$. Note that the form of square symmetry varies with off-axis alignment, β, and is summarized in Table 4.

Table 4 - Conditions for hygro-thermally curvature-stable behaviour in coupled laminates with standard ply orientations

Lamination parameters and stiffness relationships with respect to material axis alignment, β.		
$\beta = m\pi/2$	$\beta = \pi/8 + m\pi/2$ ($m = 0, 1, 2, 3$)	$\beta \neq m\pi/2, \pi/8 + m\pi/2$
(A_S) $\begin{bmatrix} A_{11} & A_{12} & 0 \\ A_{21} & A_{11} & 0 \\ 0 & 0 & A_{66} \end{bmatrix}$ $\boldsymbol{\xi_1} = \boldsymbol{\xi_3} = \xi_4 = 0$		(A_F) $\begin{bmatrix} A_{11} & A_{12} & A_{16} \\ A_{21} & A_{11} & -A_{16} \\ A_{16} & -A_{16} & A_{66} \end{bmatrix}$ $\boldsymbol{\xi_1} = \boldsymbol{\xi_3} = 0$
(B_S) $\begin{bmatrix} B_{11} & -B_{11} & 0 \\ -B_{11} & B_{11} & 0 \\ 0 & 0 & -B_{11} \end{bmatrix}$ $\boldsymbol{\xi_5} = \boldsymbol{\xi_7} = \xi_8 = 0$	(B_t) $\begin{bmatrix} 0 & 0 & B_{16} \\ 0 & 0 & -B_{16} \\ B_{16} & -B_{16} & 0 \end{bmatrix}$ $\boldsymbol{\xi_5} = \xi_6 = \boldsymbol{\xi_7} = 0$	(B_F) $\begin{bmatrix} B_{11} & -B_{11} & B_{16} \\ -B_{11} & B_{11} & -B_{16} \\ B_{16} & -B_{16} & -B_{11} \end{bmatrix}$ $\boldsymbol{\xi_5} = \boldsymbol{\xi_7} = 0$

The thermal load vector is also square symmetric for both laminates, which equates to thermally isotropic behaviour (Verchery, 2011a), and the thermal moment vector is null:

$$N^{th} = \begin{Bmatrix} N_x^{th} \\ N_y^{th} \\ N_{xy}^{th} \end{Bmatrix} = \frac{1}{2}\begin{Bmatrix} U_1^{th} \\ U_1^{th} \\ 0 \end{Bmatrix}\Delta T \qquad M^{th} = \begin{Bmatrix} M_x^{th} \\ M_y^{th} \\ M_{xy}^{th} \end{Bmatrix} = \begin{Bmatrix} 0 \\ 0 \\ 0 \end{Bmatrix} \tag{9}$$

Figures 5 and 6 shows polar plot of the **ABD** matrix for laminates 25 and 27, normalized against the equivalent (thickness) isotropic laminate, i.e.:

$$A_{Iso} = E_{Iso}H/(1 - \nu_{Iso}^2) = U_1H \tag{10}$$

$$B_{Iso} = E_{Iso}H^2/4(1 - \nu_{Iso}^2) = U_1H^2/4 \tag{11}$$

$$D_{Iso} = E_{Iso}H^3/12(1 - \nu_{Iso}^2) = U_1H^3/12 \tag{12}$$

noting that B_{Iso} represents the square symmetric form shown in the first column of Table 4 and the two figures that follow are graphical representations of the variations in the matrices shown in adjacent columns.

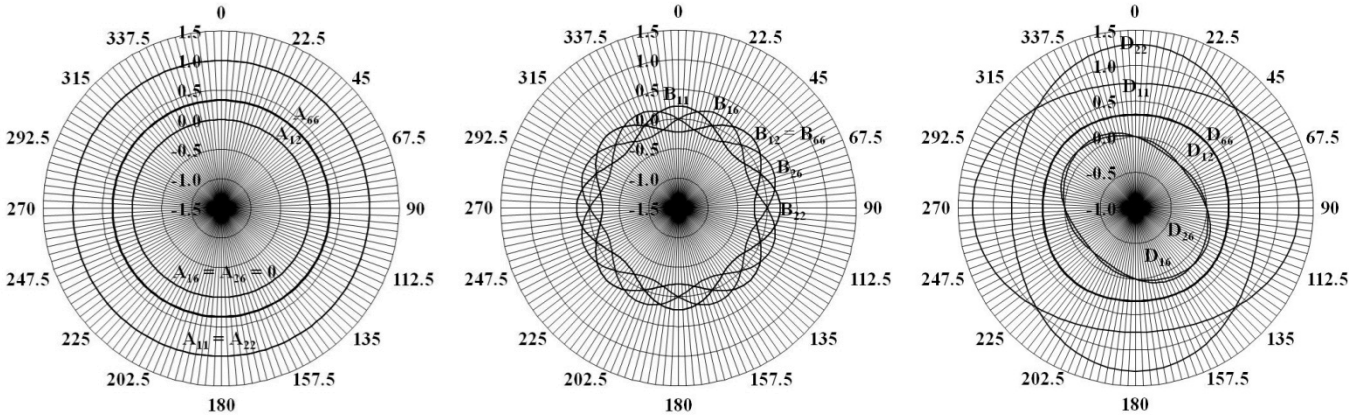

(a) A_{ij}/A_{Iso} (b) B_{ij}/B_{Iso} (c) D_{ij}/D_{Iso}

Figure 5 – Polar plots of the: (a) **A**; (b) **B** and (c) **D** matrices corresponding to off-axis material alignment, $0° \le \beta \le 360°$, for laminate 25: $[-/+_3/O/-_2/+/●_3/O_2]_T$, assuming standard ply orientations ±45, 0 and 90° in place of symbols +, –, O and ●, respectively.

In view of the test results that follow, the form of the **ABD** matrix of interest relates to the off-axis alignment $\beta = \pi/8$, or 22.5°, since this gives rise to coupling between extension and twisting; for which an experimental test is available to assess the magnitude of this form of mechanical coupling behaviour.

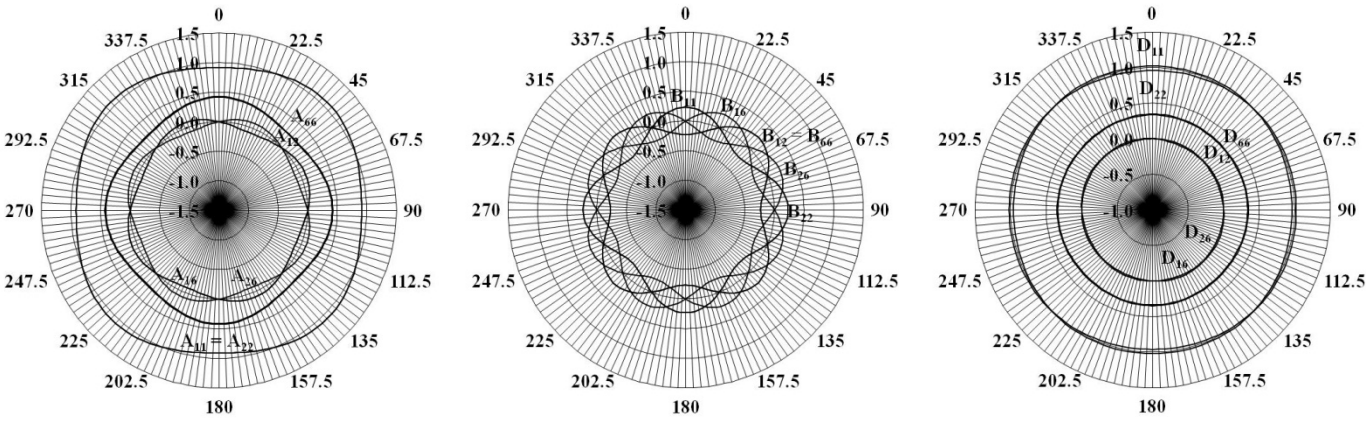

(a) A_{ij}/A_{Iso} (b) B_{ij}/B_{Iso} (c) D_{ij}/D_{Iso}

Figure 6 – Polar plots of the: (a) **A**; (b) **B** and (c) **D** matrices, corresponding to off-axis material alignment, $0° \le \beta \le 360°$, for laminate 27: $[-/+/+/-/+/-/-/+/●/○/○/●]_T$, assuming standard ply orientations ±45, 0 and 90° in place of symbols +, –, ○ and ●, respectively. Note that bending stiffness closely approximates isotropic behaviour in this case.

III. Experiment Setup and Finite Element Modelling.

Laminated plates (380mm square) were manufactured by Airbus using a proprietary unidirectional carbon-fibre/epoxy material and high temperature/pressure cure cycle. Specimens of dimensions 24mm × 240mm were then cut at off-axis orientation, $\beta = 22.5°$; the angle required to provide mechanical extension-twisting coupling, see Table 4.

An Instron E10000 tension-torsion test rig, see Fig. 7, was employed to assess the magnitude of the extension-twisting coupling for each specimen. The tests were performed under load control, maintaining zero torque, up to a maximum tensile load of 2,225N, using load increments of 445N, thus allowing the linearity of twist angle variation to be assessed.

Figure 7 - Testing of the specimen using an Instron E10000 tension-torsion machine.

A finite element (ABAQUS) simulation of the mechanical extension-twisting behaviour was performed using a nonlinear (geometry) analysis. The specimen was modelled with thin shell (S8R5) elements; 5 elements across the width and 38 elements along the length of the specimen were sufficient to provide good convergence; the boundary conditions were applied via rigid body elements to a reference node at which the load was applied and axial extension and rotation measured.

IV. Results and Discussion.

Table 5 gives the form of the mechanical coupling in both laminates as a result of the off-axis orientation, $\beta = 22.5°$, of the principal material axis of the specimens with respect to the loading axis. Note that isotropic extensional stiffness properties ($\mathbf{A}_I$) of laminate 25 are constant for all axis orientations.

Figure 8 illustrates the Extension-Twisting coupling behaviour of the two laminate classes. The results of the experimental tests are presented together with the finite element simulation results for direct comparison.

Table 5 – Coupling characteristics for laminates 25 and 27 with off-axis alignment, $\beta = 22.5°$.

	$\beta = 22.5°$
Laminate 25	$A_I B_t D_F$: *E-T-S-B*;*B-T*
Laminate 27	$A_F B_t D_F$: *E-S*; *E-T-S-B*;*B-T*

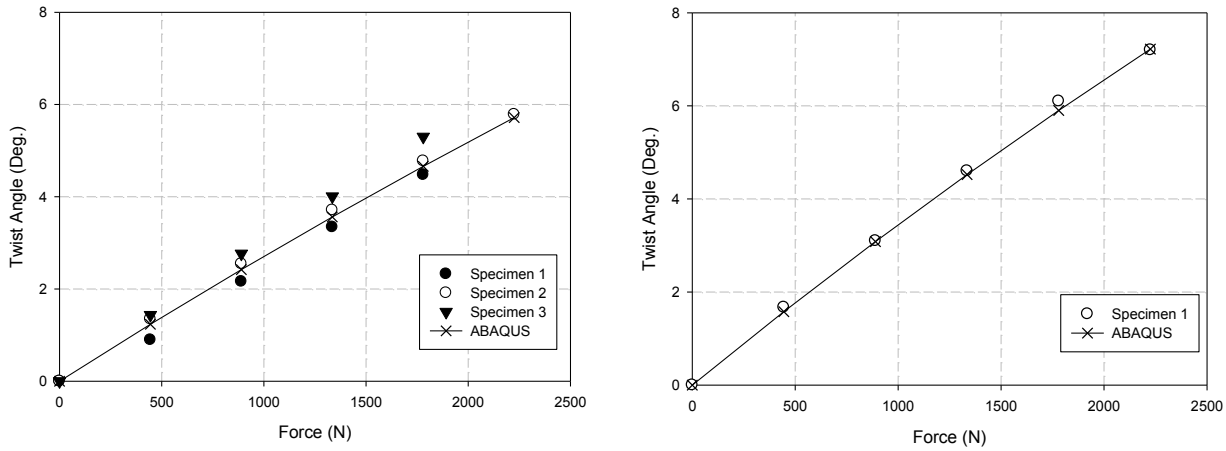

(a) (b)

Figure 8 - Comparison between Experimental and ABAQUS results for: (a) Laminate 25 and; (b) Laminate 27.

Figure 8 demonstrates that the finite element simulations are in good agreement with the experimental results. At maximum load (2,225N) these results equate to a twist angle of 5.8° and 7.2° over a gauge length of 170mm, for laminates 25 and 27, respectively.

V. Concluding remarks

An assessment of the structural response of hygro-thermally curvature-stable (HTCS) laminates with exotic mechanical coupling behaviour has been reported. Preliminary experimental results have been presented for laminates with extension-twisting coupling behaviour and have been shown to demonstrate excellent agreement with non-linear (geometry) finite element predictions.

Acknowledgments

Airbus (Hamburg and Composites Centre Stade, Germany), and in particular Björn Stephan & Hauke Schultz, are gratefully acknowledged for manufacturing 30 proof of concept specimens which made this study possible. Philip Riches and Richard Black from the University of Strathclyde are also gratefully acknowledged for supporting the test program.

References

Chen, H. P. (2003). *Study of Hygrothermal Isotropic Layup and Hygothermal Curvature Stable Coupling Composite Laminates.* Proc. 44th AIAA/ASME/ASCE/AHS/ACS Structures, Structural Dynamics, and Materials Conference, Paper No. AIAA-2003-1506, Longbeach, CA, USA.

Cross, R. J., Haynes, R. A., & Armanios, E. A. (2008). Families of Hygrothermally Stable Asymmetric Laminated Composites. *Journal of Composite Materials, 42*(7), 697-716.

ESDU. (1994). Stiffnesses of laminated flat plates *Engineering Science Data Unit, Item No. 94003*, 1-28.

Nixon, M. W. (1987). *Extension-twist coupling of composite circular tubes with application to tilt rotor blade design*. Proc. 28th AIAA/ASME/ASCE/AHS/ASC Structures, Structural Dynamics, and Materials Conf., Paper No. AIAA-87-0772, Monterey, USA.

Tsai, S. W., & Hahn, H. T. (1980). *Introduction To Composite Materials*: Technomic Publishing Company, Inc.

Verchery, G. (2011a). Design Rules for the Laminate Stiffness. *Mechanics of Composite Materials*, 47(1), 47-58.

Verchery, G. (2011b). *Thermally Stable Laminates*. Proc. 18th International Conference on Composite Materials, Paper No. IF0797, Jeju Island, Korea.

Winckler, S. J. (1985). Hygrothermally curvature stable laminates with tension-torsion coupling. *Journal of the American Helicopter Society, 30*, 56-58.

York, C. B. (2008). *On composite laminates with extensional-anisotropy*. Proc. 49th AIAA/ASME/ASCE/AHS/ASC Structures, Structural Dynamics, and Materials Conf., Paper No. AIAA-2008-1752, Schaumburg, USA.

York, C. B. (2009). Characterization of non-symmetric forms of fully orthotropic laminates, AIAA J. Aircraft, 46(4), 1114-25.

York, C. B. (2010). Unified approach to the characterization of coupled composite laminates: Benchmark configurations and special cases. *Journal of Aerospace Engineering, 23* (4), 219-242.

York, C.B. (2011a). Coupled quasi-homogeneous orthotropic laminates. *Mechanics of Composite Materials*, 47(4) pp. 405-426.

York, C.B. (2011b). Unified approach to the characterization of coupled composite laminates: Hygro-thermally curvature-stable configurations. *International Journal of Structural Integrity*. 2(4).

York, C.B. (2011c). *Hygro-thermally curvature-stable laminates with non-standard ply orientations*. Proc. 18th International Conference on Composite Materials, Paper No. IF1966, Jeju Island, South Korea.